applied sciences

MDPI

Article

Hybrid Geopolymer Composites Based on Fly Ash Reinforced with Glass and Flax Fibers

Hana Šimonová [1], Patrycja Bazan [2,*], Barbara Kucharczyková [1], Dalibor Kocáb [1], Michał Łach [2], Dariusz Mierzwiński [2], Kinga Setlak [2], Marek Nykiel [2], Przemysław Nosal [3] and Kinga Korniejenko [2,*]

[1] Faculty of Civil Engineering, Brno University of Technology, Veveří 331, 60200 Brno, Czech Republic; hana.simonova@vut.cz (H.Š.); barbara.kucharczykova@vut.cz (B.K.); dalibor.kocab@vutr.cz (D.K.)
[2] Faculty of Material Engineering and Physics, Cracow University of Technology, Warszawska 24, 31-155 Cracow, Poland; michal.lach@pk.edu.pl (M.Ł.); dariusz.mierzwinski@pk.edu.pl (D.M.); kinga.setlak@pk.edu.pl (K.S.); marek.nykiel@pk.edu.pl (M.N.)
[3] Faculty of Mechanical Engineering and Robotics, AGH University of Krakow, Mickiewicza 30, 30-059 Cracow, Poland; pnosal@agh.edu.pl
* Correspondence: patrycja.bazan@pk.edu.pl (P.B.); kinga.korniejenko@pk.edu.pl (K.K.)

Featured Application: Building materials for products with lower carbon footprints and increased mechanical properties.

Abstract: This article's aim is to analyze physical, mechanical, and fracture properties as well as the thermal investigation of geopolymer composites reinforced with flax, glass fiber, and also the hybrid combination of fibers. Two types of matrices were considered as composites matrices. The first composition was based on fly ash and river sand. The second matrix composition contained fly ash and glass spheres. The content of reinforcement was 1% by mass. Compressive strength and three-point bending fracture tests were performed. The values of fracture toughness and fracture energy were determined. The resonance method was used to verify the dynamic characteristics, such as the dynamic modulus of elasticity and the dynamic Poisson ratio. The results show that single-type fibers in composites based on fly ash and glass spheres did not affect compressive strength. However, introducing hybrid reinforcement increased compressive strength by about 10% compared to the reference specimens. Flax fibers and hybrid reinforcement ensured higher fracture toughness and energy. The results also revealed great potential for glass sphere application to geopolymer materials in terms of fracture mechanics and thermal properties. Despite the lower strength properties in relation to geopolymers based on sand aggregate, applying reinforced fibers into the composite with glass spheres enhanced the compressive strength compared to other materials. Materials modified with glass spheres have a thermal conductivity twice as low as that of materials containing river sand.

Keywords: geopolymer composites; cracking mechanics; natural fibers; glass fibers; glass spheres

Citation: Šimonová, H.; Bazan, P.; Kucharczyková, B.; Kocáb, D.; Łach, M.; Mierzwiński, D.; Setlak, K.; Nykiel, M.; Nosal, P.; Korniejenko, K. Hybrid Geopolymer Composites Based on Fly Ash Reinforced with Glass and Flax Fibers. *Appl. Sci.* **2024**, *14*, 9787. https://doi.org/10.3390/app14219787

Academic Editor: Giuseppe Lacidogna

Received: 15 September 2024
Revised: 16 October 2024
Accepted: 24 October 2024
Published: 26 October 2024

1. Introduction

Geopolymer materials have gained great interest as a new generation of environmentally friendly building materials in relation to ones based on ordinary Portland cement (OPC). They are characterized by an amorphous or partially crystalline structure resulting from silicon, aluminum, and oxygen condensation polymerization. The polymerization reaction takes place due to alkaline activation. Geopolymers have better fire resistance, acid resistance, and comparable strength properties than composites based on OPC. As a potential application of geopolymers, construction materials or materials for the utilization and immobilization of toxic/radioactive substances are often indicated [1–4]. Fly ash, metakaolin, clay, red mud, silica fume, and volcanic rock are the most used precursors for geopolymers [5]. To produce a geopolymer composite that meets the strength requirements, the most common addition as an aggregate is sand. The introduction of aggregate with

different gradations aims to ensure mechanical properties, and volumetric stability, and reduce the price of the material. Usually, river sand is introduced as an aggregate, although research on the application of dune sands was also conducted. Still, this material with small gradations caused a decrease in compressive strength, mainly if this type of addition constituted one hundred percent of the aggregate portion [6]. Geopolymers contained in river sand are characterized by accelerated setting, higher mechanical properties, better compatibility and workability, lower water absorption, and similar shrinkage compared to only fly ash-based geopolymers. However, the introduction of sand into the geopolymer deteriorates properties such as leachability chlorides and the durability of the material [7]. Scientific research has shown that the greater the amount of the aggregate, the better the strength properties of geopolymers. However, the research presented in the literature indicates that the optimization of the volume of river sand or adaptation of other process waste can effectively positively affect the properties of geopolymer materials and thus reduce the consumption of natural mineral resources [8–10]. Glass spheres are one of the additives introduced to geopolymer for building materials to produce insulating materials. The introduction of glass spheres into geopolymers causes a decrease in the density of the material, and provides satisfactory strength properties and adequate thermal insulation, significantly reducing the thermal conductivity of materials. Both solid materials, in foamed form and thermal coatings modified with glass spheres, were investigated. Each time, these materials demonstrated that they developed thermal comfort and reduced energy consumption [11–15].

As a reinforcement of geopolymers, organic and inorganic fibers are often implemented. The application of inorganic fibers dates back to the last decades and aims to develop high-performance materials that meet structural requirements. The most commonly used inorganic fibers include carbon, aramid, polyethylene, glass, basalt, boron, boron carbide, boron nitride, zirconium oxide, silicon carbide, and silicon nitride. The addition of inorganic fibers significantly improves the physical, mechanical, and thermal properties of composites [16]. Glass fiber is one of the most critical reinforcements of different composites. The benefits of the usage of glass fibers are, i.a., improvement of tensile strength and low production costs. The structure of the glass fibers is amorphous, and Young's modulus of the glass fiber is the same as that of bulk glass. They increase the stiffness and reduce the deformability of the composites. They are also characterized by good thermal insulation properties. The main disadvantages of glass fibers are relatively reduced long-term strength, and poor resistance to moisture and alkaline media. Glass fibers introduced into geopolymers cause an increase in flexural and compressive strength and an enhancement in Young's modulus of composite. However, these properties depend on the amount and type of applied fibers. An increase in the aging resistance of geopolymer materials containing glass fibers was also observed concerning materials without reinforcement, which indicates an improvement in long-term strength [17–21]. Natural fibers are being increasingly applied as the advantages of natural fibers are their biodegradability, renewability, relatively high strength properties, and no negative environmental impact. Since geopolymer materials are produced at a relatively low temperature, not exceeding 80 °C, there is a growing interest in using natural fibers to reinforce geopolymer composites. The most commonly introduced natural fibers include coconut, cotton, flax, hemp, jute, kenaf, sisal, abaca, banana, and palm. Natural fibers have significant advantages over synthetic fibers but are not free from disadvantages. Due to the structure of natural fibers (lignin and hemicellulose and the resulting hydroxyl groups), these materials are affected by moisture. They also have low dimensional stability and low fire resistance [22]. Flax fibers are natural fibers that belong to one of the strongest fibers related to their low density. The strength of flax fibers can reach over 2 GPa, with deformation up to about 4%. Still, these properties depend on the plant variety, length, and diameter of the fibers, the processing parameters, the applied finishing, and any defects on the surface [23]. Studies on composites reinforced by flax fibers have presented significant improvement in strengthening geopolymers during flexural loading by about 20–30%. However, properties that strongly

depend on used fibers may also reduce the compressive and tensile strength. The decrease in mechanical properties is connected with the increase in porosity of the geopolymer (which acts as a stress concentrator). However, scientific research has proven the advantage of using flax fibers as a reinforcing material for geopolymers and eco-friendly additives obtained from renewable sources. The study pointed out that the porosity can be minimized by appropriate surface treatment, increasing workability, or being considered a naturally occurring structure with better thermal and acoustic properties [24–28]. Intensive research on geopolymer composites with organic and inorganic reinforcements has revealed the advantages and disadvantages of geopolymer materials. The disadvantages of geopolymers include a brittle structure and lower tensile strength, so the introduction of reinforcement is a promising solution. The fibers and particles distributed in the geopolymer matrix are designed to couple cracks and reduce the tendency of cracks to propagate. Extensive research demonstrates the need to address the identified issues. Geopolymer composites with hybrid fiber–fiber reinforcement are intensively produced and examined. Examples of this type of reinforcement can be the combination of steel fiber with polypropylene fiber, basalt fiber with polypropylene, steel fiber with Kevlar fiber, and many others. Research on hybrid reinforced composites has shown an increase in the compressive strength, tensile strength, and impact strength of this type of material [29–35]. Research on these material types is of great importance for filling the gap in knowledge regarding the reduction in the brittleness of geopolymer composites. Overcoming these limitations would result in greater use of geopolymer materials as structural and building materials.

In the literature, there is only a little research on hybrid fibers in lightweight materials. They show that the synergy effect between the fibers can bring significant improvement to the composite. The motivation for undertaking this topic was to improve the mechanical properties of lightweight geopolymer composites using hybrid fibers. This work aims to analyze the mechanical and fracture properties of geopolymer composites with single-type and hybrid reinforcement. Such tests allow for assessing the suitability of synthetic fibers and natural fibers as a reinforcement of materials characterized by resistance to brittle cracking. Furthermore, such analysis can help predict the mechanical behavior of geopolymer composites in the construction sector. In this study, glass fibers and flax fibers were selected. Glass fibers are one of the most popular fibers used in building materials because of the good ratio between the price and obtained properties. As natural fibers, flax fibers were applied because they are renewable, light fibers that naturally occur in Poland and the Czech Republic.

2. Materials and Methods

2.1. Materials

Geopolymers were made using an alkaline promoter based on sodium, fly ash (bulk density—1.1 g/cm^3) (Elektrocieplownia Skawina, Skawina, Poland), and river sand (bulk density—1.52 g/cm^3) or glass spheres (BIOSPACE, diameter around 0.1 mm). Glass fibers (Krosglass S.A., Poland, length ~3 mm, diameter ~10 µm, density—2.7 g/cm^3, Young's modulus ~70 GPa) and flax fibers (Hempiflax Group Sp. Z o.o., Poland, length ~5–10 mm, diameter 40 to 80 µm, density—1.5 g/cm^3, Young's modulus ~60 GPa) were used as reinforcement. The short fibers were selected because they have advantages in processing and allow for the use of traditional methods, the same properties as for pure matrix materials. In this study, we also selected the shortest available fibers, taking into account the laboratory scale of our experiment. In the case of natural fibers, it is not possible to obtain the fibers with strict dimensions, because they are obtained in the process of plant growth. For the study, we select the shortest fibers available on the market.

For the activation process, a 10-molar (10 M) solution of sodium hydroxide NaOH in combination with a solution of sodium silicate (water glass with a modulus of 2.5 molar and a density of about 1.45 g/cm^3) in a ratio of 1:2 was used. This solution was prepared by adding an aqueous solution of sodium silicate and water to the solid sodium hydroxide. The solution was allowed to equilibrate to ambient temperature before use. The first stage

of manufacture was mixing dry ingredients: fly ash, aggregate, and reinforcing fibers, then adding an alkaline solution and continuing mixing until a homogeneous mass was achieved. The prepared mass placed in molds was subjected to vibrations to remove air bubbles on a vibrating table. The next step was to put them in a laboratory dryer (SLW 750 STD, POL-EKO-APARATURA, Wodzisław Śląski, Poland) for 24 h at a temperature of 75 °C and atmospheric pressure. After that, specimens were stored under laboratory conditions until the tests were performed.

The histograms of the grain distribution and the curve of the cumulative grain distribution of materials are presented in Figure 1. Table 1 shows the particle size distribution of applied raw materials, and Table 2 describes the composition of the produced geopolymer composites.

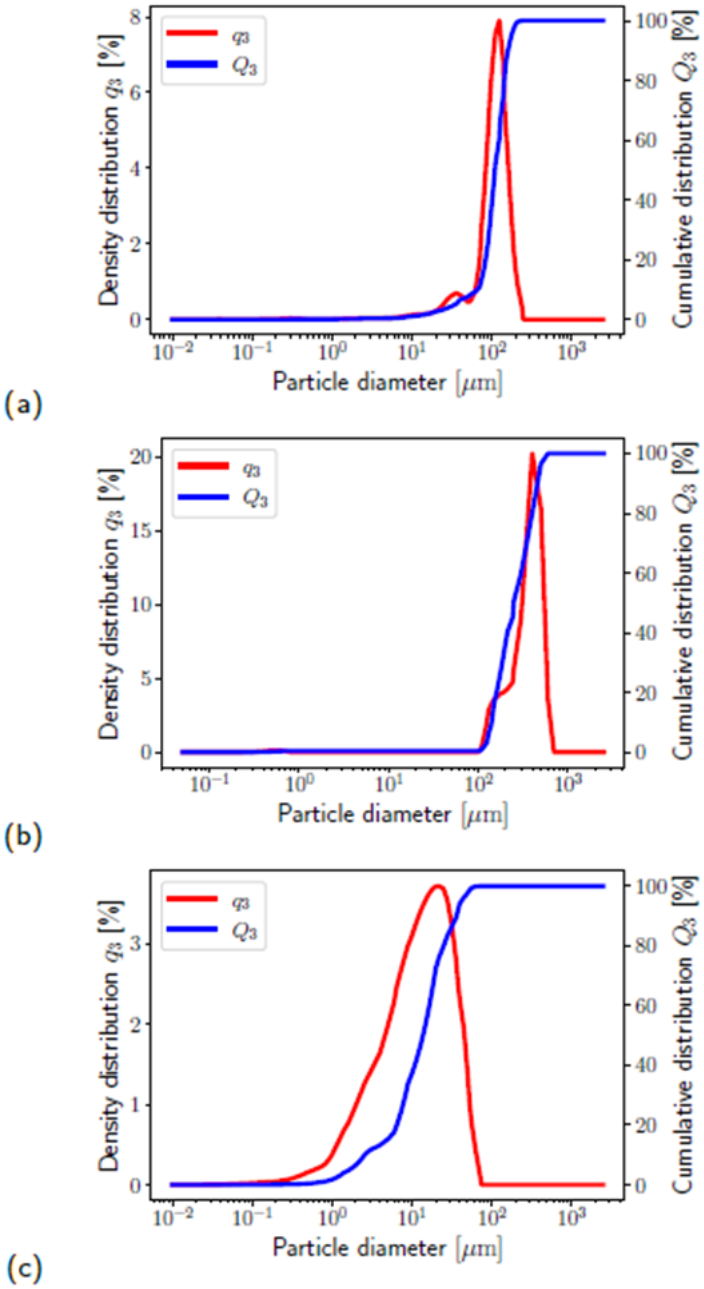

Figure 1. Particle size distribution of glass sphere (**a**), river sand (**b**), and fly ash (**c**).

Table 1. Distribution of particle size of applied raw materials.

D-Values [μm]	Fly Ash	River Sand	Glass Sphere
D_{10}	2.210	173.235	41.944
D_{50}	11.892	342.393	108.735
D_{90}	34.414	474.750	169.308
Mean size	16.273	376.308	110.640
SPAN *	2.708	0.881	1.079
D, [5.3] **	21.183	396.066	119.170

* Span = $(D_{90} - D_{10})/D_{50}$, ** The volume-weighted mean area size.

Table 2. Designation of manufactured composites.

Designation	Mixture Proportion [% by Weight]				
	Fly Ash	Sand	Glass Sphere	Glass Fibers	Flax Fibers
S_REF	50	50		-	-
GS_REF	50		50		
S_GF	49.5	49.5		1.0	-
GS_GF	49.5		49.5	1.0	
S_FF	49.5	49.5		-	1.0
GS_FF	49.5		49.5		1.0
S_MIX	49.5	49.5		0.5	0.5
GS_MIX	49.5		49.5	0.5	0.5

The particle size of the base materials significantly affects the physical and mechanical properties of geopolymer materials. The smaller the particle sizes of ashes intended for geopolymer synthesis, the greater their reactivity during the geopolymerization process. Smaller particle sizes have increased active surfaces, which promotes a faster dissolution reaction and the formation of a geopolymer gel in condensation polymerization [11].

Table 3 shows the results of the X-ray analysis of the used fly ash. Based on diffraction tests, quartz and mullite and a small amount of anhydrite and hematite characterized the fly ash.

Table 3. X-ray analysis of fly ash.

Material	Identified Phase		Percentage Range, %
	Phase	Chemical Formula	
Fly ash	Quartz	SiO_2	43.3
	Mullite	$Al_6Si_2O_{13}$	53.8
	Hematite	Fe_2O_3	0.7
	Magnetite	Fe_3O_4	0.3
	Anhydrite	$CaSO_4$	1.5
	Rutile	TiO_2	0.4

The phases of the materials present in the fly ash belong to the crystalline phases. It is worth noting that some studies of geopolymer materials indicate that even a small amount of quartz may positively affect mechanical properties. In contrast, the presence of other minerals may have opposite effects. An example is illite, which causes changes in geopolymer morphology and leaching behavior [36–38]. The investigated fly ash has a large number of quartz and mullite which allows us to use it in the geopolymerization process.

2.2. Methods

2.2.1. Raw Material Analysis

Particle size analysis of fly ash, river sand, and glass spheres was carried out on the Anton Paar PSA 1190 LD Graz particle analyzer (Anton Paar GmbH, Graz, Austria). The study was performed using the laser diffraction method.

X-ray diffraction (XRD) was performed by using a PANalytical laboratory device (PANalytical, Almelo, The Netherlands). The main aim was to analyze the mineral composition. The analysis took place on powdered samples. The phase composition was determined by using the Debye–Scherrer method. Phase analysis was performed using Cu-Kα radiation. Phase identifications were based on the evaluation of interplanar distances using the HighScore Plus software (V5.2) with the PDF4+ database provided by the International Center for Diffraction Data (ICDD). It is a technique that allows us to determine the phase composition and crystal structure of the tested material. The analysis consists of X-ray diffraction as it passes through the test sample. Diffractions reveal information about the distance of the atomic layers of the sample—based on which the structure is determined.

2.2.2. Thermal Conductivity

The thermal conductivity test was performed in accordance with ASTM C518 (https://www.astm.org/c0518-21.html, accessed on 23 October 2024) JIS A1412 (https://www.intertekinform.com/en-gb/standards/jis-a-1412-1-1999-623369_saig_jsa_jsa_1436257/, accessed on 23 October 2024), ISO 8301 (https://www.iso.org/standard/15421.html, accessed on 23 October 2024), and DIN EN 12667 (https://www.en-standard.eu/din-en-12667-thermal-performance-of-building-materials-and-products-determination-of-thermal-resistance-by-means-of-guarded-hot-plate-and-heat-flow-meter-methods-products-of-high-and-medium-thermal-resistance-english-version-of, accessed on 23 October 2024) on the HFM 446 Lambda Series from NETZSCH (Netzsch GmbH & Co., Selb, Germany). Measurements were carried out for the temperature range of 0–20 °C. The measurement was made using the method of flat surfaces. Panels measuring approximately 200 × 200 × 25 mm were made for the tests. For the test on the machine, two different temperatures were set at the bottom and top of the panel. The panel was tested until determining the time at which the temperatures were equal. After starting the measurement, the process of stabilization of the system took place—the temperature on both sides of the tested specimen was balanced. Using the formulas for heat resistance, temperature gradient, and thermal conductivity coefficient, the values of these indicators were calculated for each specimen. Thermal conductivity is the amount of thermal energy passing through a specific mass of the specimen. According to the second law of thermodynamics, heat always flows towards the area of lower temperature.

This is expressed by the coefficient of thermal conductivity:

$$\lambda = Q \times L \times A \times \Delta T \quad (1)$$

where

λ—thermal conductivity,
Q—heat flux penetrating the specimen,
L—length of the specimen,
A—cross-sectional area of the specimen,
ΔT—temperature difference.

2.2.3. Microstructure Investigation

Microscopic observations were performed on a Joel JSM-820 scanning electron microscope with an EDS X-ray detector (IXRF, Inc., Austin, TX, USA). SEM analysis was carried out on the samples after mechanical strength tests were provided at least 28 days after the production of geopolymer materials.

2.2.4. Mechanical Properties, Including Fracture Behavior Analysis

The resonance method was used to determine the dynamic characteristics of investigated composites before fracture tests were conducted. The prismatic specimens with a nominal dimension of 40 × 40 × 160 mm were used. The natural frequency of longitudinal and torsional vibrations was assessed using a Handyscope HS4 oscilloscope (TiePie engineering, Sneek, The Netherlands) with an acoustic sensor [39]. The absolute values

of the dynamic modulus of elasticity and the dynamic Poisson ratio were calculated in compliance with the ASTM C215-19 [40].

Three-point bending (3PB) tests were performed for the above-mentioned prismatic specimens to determine the selected mechanical fracture characteristics of the investigated geopolymer composites. An initial notch was made one day before fracture tests. A diamond blade saw made the central edge notch with a nominal depth of about 1/3 of the specimen's height. The span length was set to 120 mm. The specimens were tested approximately at the age of 28 days. Fracture tests were conducted using the stiff multipurpose mechanical testing machine LabTest 6.250 (LaborTech, s.r.o., Opava, Czech Republic) with a load range of 0–250 kN. The loading process was governed by a constant increment of displacement of 0.02 mm/min during the whole course of testing. The vertical displacement (midspan deflection) d was measured using the inductive sensor mounted in a special measurement frame placed on the specimens. The outcome of each test is a vertical force F vs. d diagram. The diagrams recorded during the experiment were processed to obtain the correct input values for the consecutive evaluation of mechanical fracture parameters. The processing of diagrams covered the elimination of duplicate points, the shifting of the origin of the coordinate system, the smoothing of the diagram, and the reduction in the number of points. The processing of recorded diagrams was performed in GTDiPS software (v2t53i) [41] which is based on advanced transformation methods used for the processing of extensive point sequences. The $F-d$ diagrams from fracture tests are introduced in Figure 2. Each curve represents the response of one tested specimen. The difference in fracture response of individual specimens made of the same composite is caused by the heterogeneity of materials. Especially with the addition of fibers, the difference in the post-peak part of the $F-d$ diagrams can be seen. The addition of fibers mainly influences fracture behavior in this part of the F–d diagrams and the individual specimen response depends on the distribution of fibers in the cross-section where the crack is propagating. The F–d diagrams were used to estimate values of the modulus of elasticity, effective fracture toughness, and specific fracture energy. The modulus of elasticity E was determined from the initial part of the F–d diagrams according to Stibor [42]:

$$E = \frac{F_i}{4Bd_i}\left(\frac{S}{W}\right)^3\left[1 - 0.387\frac{W}{S} + 12.13\left(\frac{W}{S}\right)^{2.5}\right] + \frac{9}{2}\frac{F_i}{Bd_i}\left(\frac{S}{W}\right)^2 F_1(\alpha_0) \quad (2)$$

where F_i and d_i are the vertical force and midspan deflection, respectively, read from the linear part of the F–d diagram, S represents span length, and B and W are the specimen's width and height, respectively. $F_1(\alpha_0)$ is the shape function according to Karihaloo [43], and α_0 is the relative crack/notch length. The first term of the equation is calculated from the deflection of the whole cross-section (without crack/notch). The second term includes the effect of the notch depth and is based on the Castigliano principles; see Karihaloo [43] for more details.

Several adaptations of linear elastic fracture mechanics (LEFMs) have been proposed to consider the nonlinear behavior of quasi-brittle materials in an approximate manner. One representative is an effective crack model [43], in which the difference between the initial tangent stiffness and the secant stiffness of the specimen at peak load F_{max} is considered. The effective crack length a_e is obtained by extending the initial notch length a_0 to such a value that the deflection d_{Fmax} will be achieved by applying the peak load F_{max} while the value of the modulus of elasticity is constant. The effective fracture toughness value K_{Ice} was calculated using an LEFM formula according to Karihaloo [43]:

$$K_{Ice} = \frac{6M_{\max}S}{BW^2}Y(\alpha_e)\sqrt{a_e} \quad (3)$$

where $Y(\alpha_e)$ is the geometry function [43] with $\alpha_e = a_e/W$, and $M_{\max}$ is the bending moment due to the peak load $F_{\max}$ and the self-weight of the specimen.

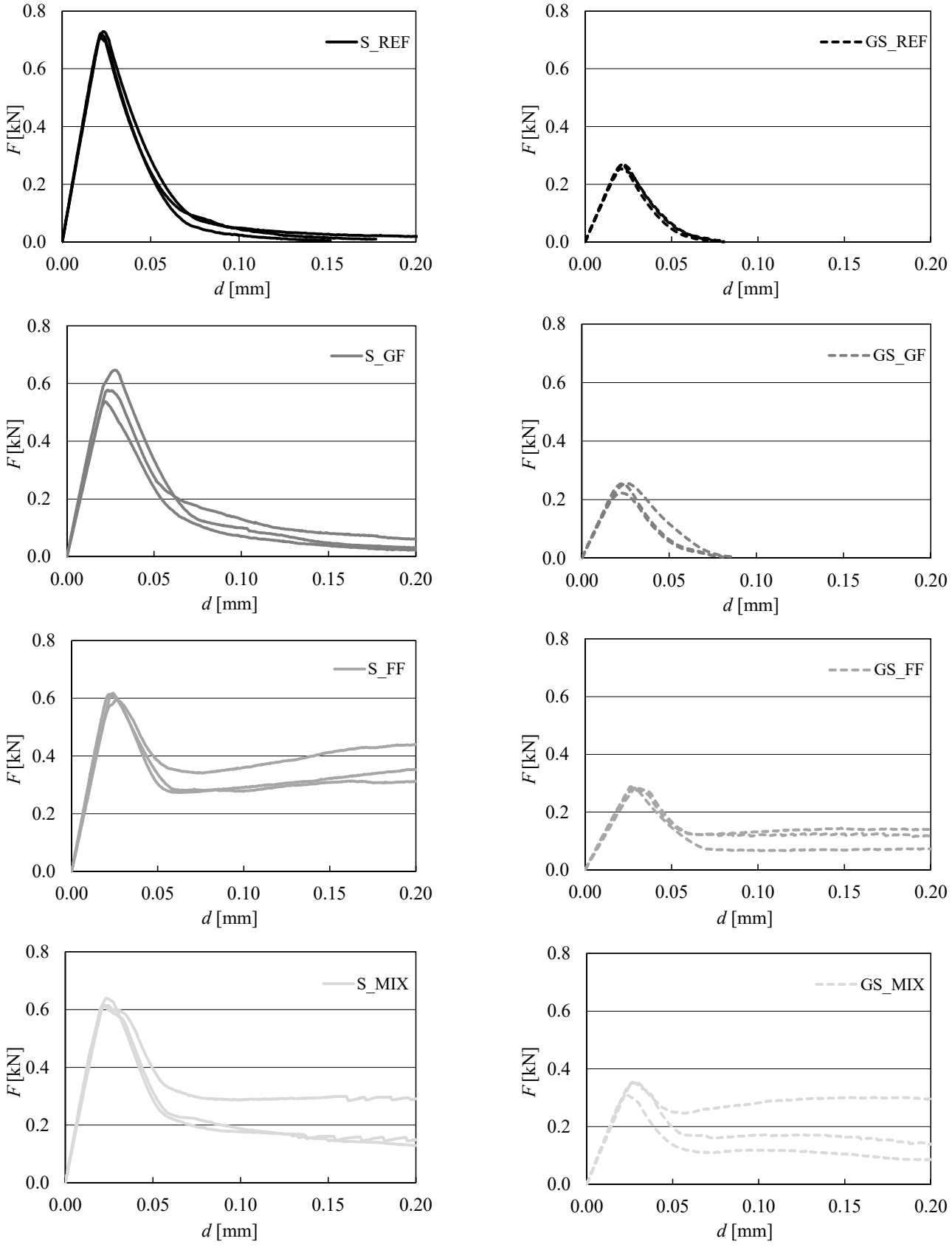

Figure 2. *F–d* diagrams of investigated geopolymer composites.

According to the RILEM recommendation [44], the specific fracture energy G_f is the average energy given by dividing the total work of fracture W_f by the projected fracture area (i.e., the area of the initially uncracked ligament):

$$G_f = \frac{W_f}{(W - a_0)B} \tag{4}$$

The value of fracture energy G_f was also investigated in two ways. At first, part $G_{f,1}$ considers the area under the F–d diagram up to the peak load F_{max}, and afterward, the area under the whole F–d diagram was considered. It should be noted that in the case of fiber-reinforced geopolymer composites, the F–d diagrams were cut at a deflection equal to 0.2 mm. It should also be noted that the informative compressive strength *fc* was determined according to ČSN EN 196-1 [45] on the fragments remaining after the fracture experiments had been conducted. The test was provided on the specimens with sizes of 40 × 40 × 40 mm. The peak load F_{max} recorded during the fracture test was used for the calculation of the informative flexural strength σ_c determined on the notched specimens (crack strength according to the terminology in the branch of fracture mechanics using ASTM E1823-20b [46]).

3. Results and Discussion

The results of the above-mentioned experiments are presented in the following figures. The mean values are represented by respective symbols according to the used aggregate (circle for river sand and square for glass spheres). The standard deviations are represented by error bars. In some cases, the coefficient of variation was low (under 5%); therefore, it is not possible to see error bars properly. Figure 3 shows the results of non-destructive measurements using the resonance method. The dynamic modulus of elasticity E_{dyn} decreased with the addition of fibers in the case of the S composite. The highest decrease was about 18% for FF addition. A slight decrease was also observed for the GS composite containing only single-type fibers, while when the MIX of fibers was used, the value increased by about 10% in comparison with the REF composite. In general, it can be stated that the dynamic modulus of elasticity is significantly lower (less than half) for all GS composites compared to S composites. This relation is connected with a reduction in the density of the materials and the same mechanical properties. Based on the results and their variability, it can be stated that the addition of single-type fibers did not influence the value of the dynamic Poisson ratio ν_{dyn} in the case of S composites. The addition of MIX fibers led to a decrease of about 20%. On the other hand, the increase in the value of the dynamic Poisson ratio for all GS composites with fibers compared to REF was observed. The highest increase of almost 50% was observed for GS with the MIX of fibers.

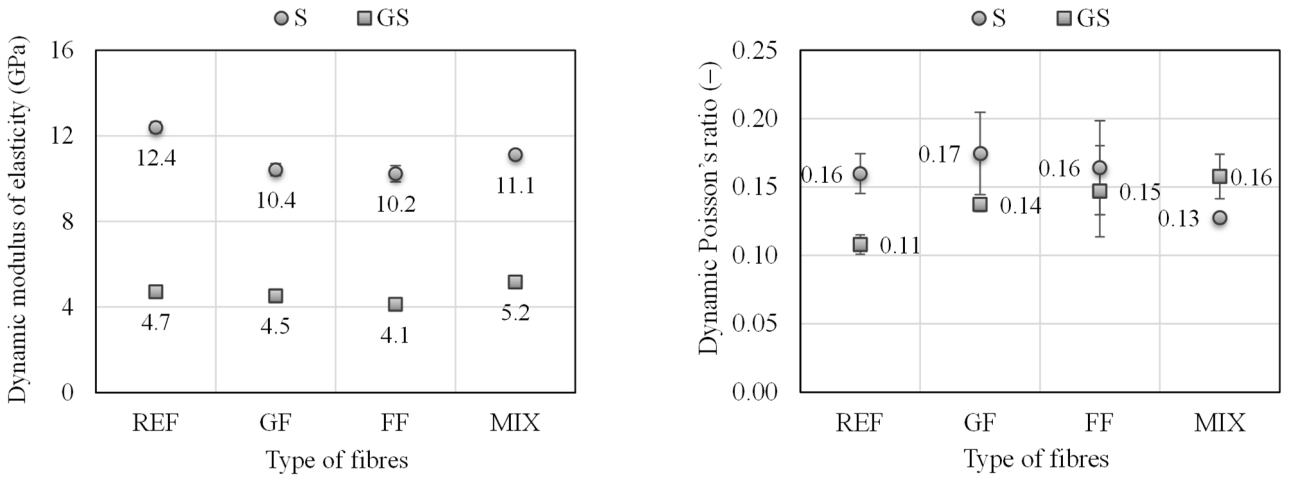

Figure 3. Mean values of dynamic characteristics of investigated geopolymer composites.

Figure 4 presents the results of basic physical and mechanical characteristics of investigated geopolymer composites with a standard deviation. In the case where the line of standard deviation is not visible, the values obtained from investigated specimens have very similar values, so the standard deviation was below 5%. The value of bulk density ρ is almost the same for all S composites, and the difference is less than 3%. In the case of the GS composite, the addition of GF did not affect bulk density; on the other hand, the addition of FF and the MIX of fibers increased the value by about 7%. The bulk density is about 45% lower in the case of GS composites in comparison with S composites.

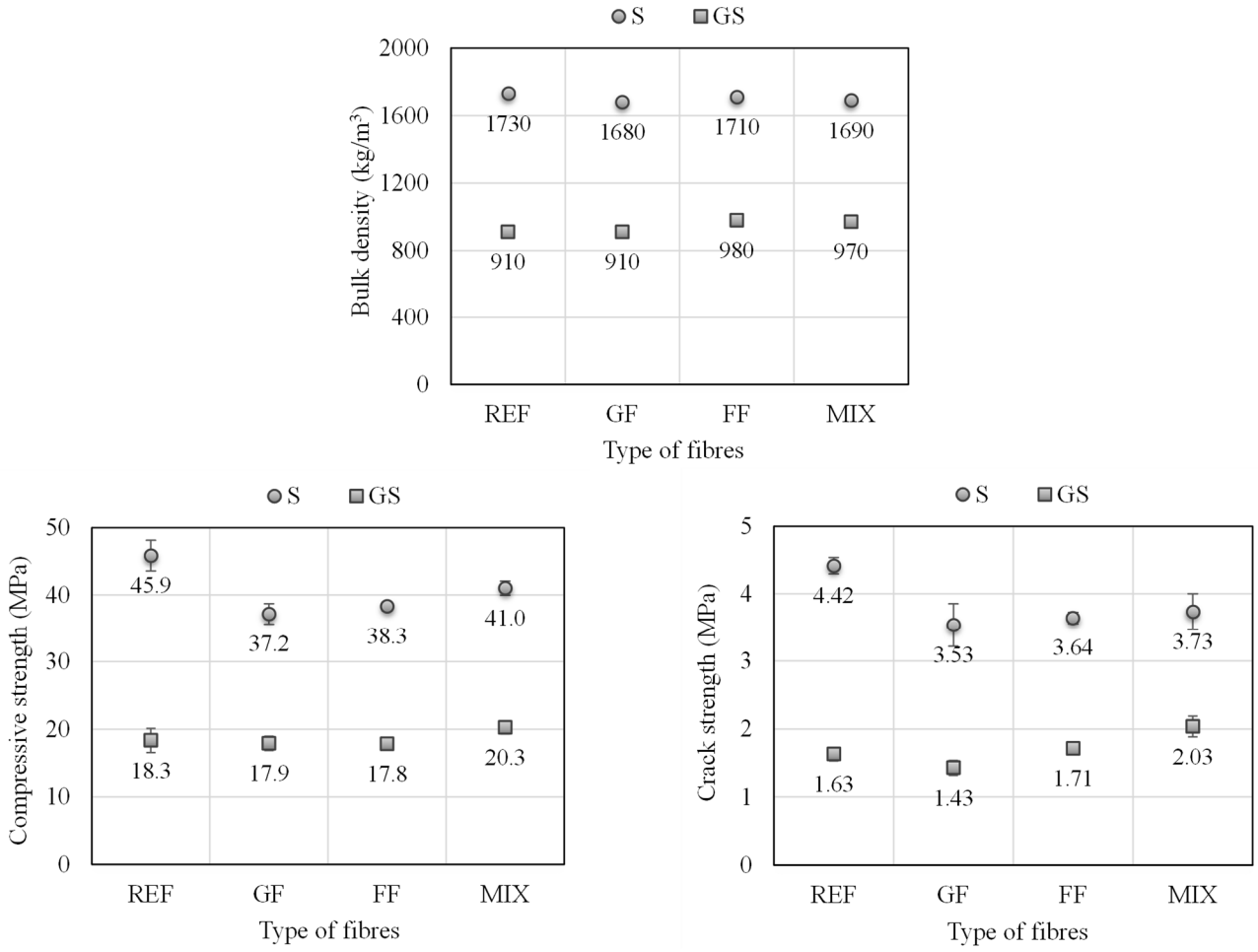

Figure 4. Mean values of basic physical and mechanical characteristics of investigated geopolymer composites.

The value of compressive strength of the S composite without fibers is about 46 MPa. It is more than two times higher compared to the GS composite. The addition of fibers caused a decrease in compressive strength in the case of the S composite. A higher decrease of about 17% was observed for S composites with single-type fibers, while when the MIX of fibers was used, the decrease was about 10%. The addition of single-type fibers did not significantly affect the compressive strength of the GS composite. When the MIX of fibers was used, an increase of about 10% was observed. The addition of fibers reduced the maximum force recorded during the fracture tests which led to a decrease of up to 20% in crack strength in the case of S composites. In the case of GS composites, the addition of GF also led to a slight decrease in crack strength. In contrast, the addition of FF and the MIX of fibers led to an increase in the value of crack strength of up to 25% when the MIX of fibers was used.

Figure 5 presents the results obtained from the evaluation of the *F–d* diagrams. The values of the modulus of elasticity show a similar trend as the values of the dynamic modulus of elasticity obtained from the resonance method for both composites. The absolute value of the static modulus of elasticity is about 15–25% higher in comparison with the dynamic one. The addition of fibers led to a decrease of about 15% in the effective fracture toughness in the case of the S composite. The addition of GF increased the variability of results in comparison with the REF composite and other types of fibers. On the other hand, in the case of the GS composite, the addition of fibers had a positive effect on the effective fracture toughness. The highest increase of about 30% was observed when the MIX of fibers was used.

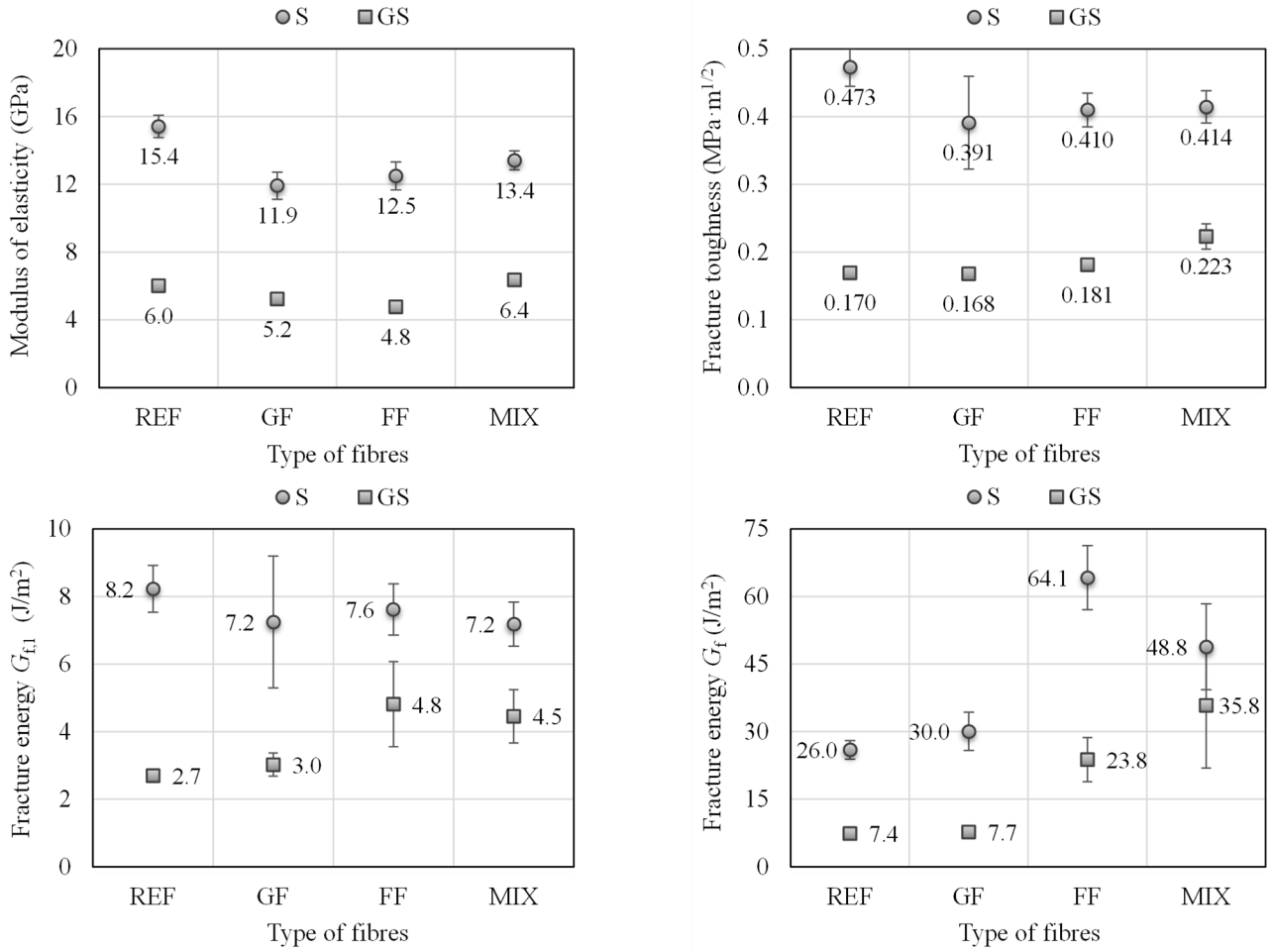

Figure 5. Values of modulus of elasticity and fracture energy for tested materials.

The last investigated parameter was specific fracture energy. At first, a part of the fracture energy $G_{f,1}$, considering the area under the *F–d* diagram up to the peak load F_{max}, is discussed. In the case of S composites, the addition of fibers caused a decrease of about 10% in comparison with REF composites. It should be noted that the variability of results is quite high when the GF was used. On the contrary, a positive effect of the addition of the fibers was observed in the case of GS composites. The addition of fibers increased the value of fracture energy in the pre-peak part of the *F–d* diagram by more than 60%. Afterward, the area under the whole *F–d* diagram was considered for evaluation. As is evident from Figure 2, the addition of FF and the MIX of fibers had a positive effect on post-peak behavior for both types of composites. The fracture energy increased more than two times and three times in the case of S and GS composites, respectively, in comparison with the REF one. The addition of fibers led to a higher variability of the results, especially

in the case of the MIX one, which could be connected with the non-uniform distribution of fibers.

Studies on the mechanical and fracture properties of geopolymer composites stated that most strength parameters increase after introducing fibers already at 0.5% by mass. Flexural strength, tensile strength, fracture toughness, and fracture energy increase in relation to reference materials. The growth in properties is attributed to the crack bridging mechanism, which contributes to larger cracks at maximum loads, with more plastic behavior resulting in increased strength and greater energy absorption capacity. The energy is usually dispersed by separating the material and overcoming the friction forces while pulling the fibers out of the matrix. The fiber bridging effect in micro- and macrocracks effectively maintains the integrity of the composite and limits catastrophic cracking. These properties, however, depend on the shape, length, and amount of introduced reinforcement and can also cause a diminishing effect in compressive strength due to an increase in the porosity of the material [47–53].

Figure 6a–d present microscopic images of composite materials based on fly ash with river sand. The microstructure analysis showed a relatively compact geopolymer structure with visible places left by undiluted fly ash particles. Cracks in the composite matrix were also visible, which indicated the brittleness of the geopolymer matrix (Figure 6a,c). The microstructure of the composite with glass fiber revealed an amorphous character with visible places of the crystal structure. Glass fibers were pretty well placed in the composite matrix, but they presented an agglomeration character. In the case of the microstructure of composites with flax fiber, a typical surface of natural fibers embedded in the composite matrix with local cracks deep into the material could be observed.

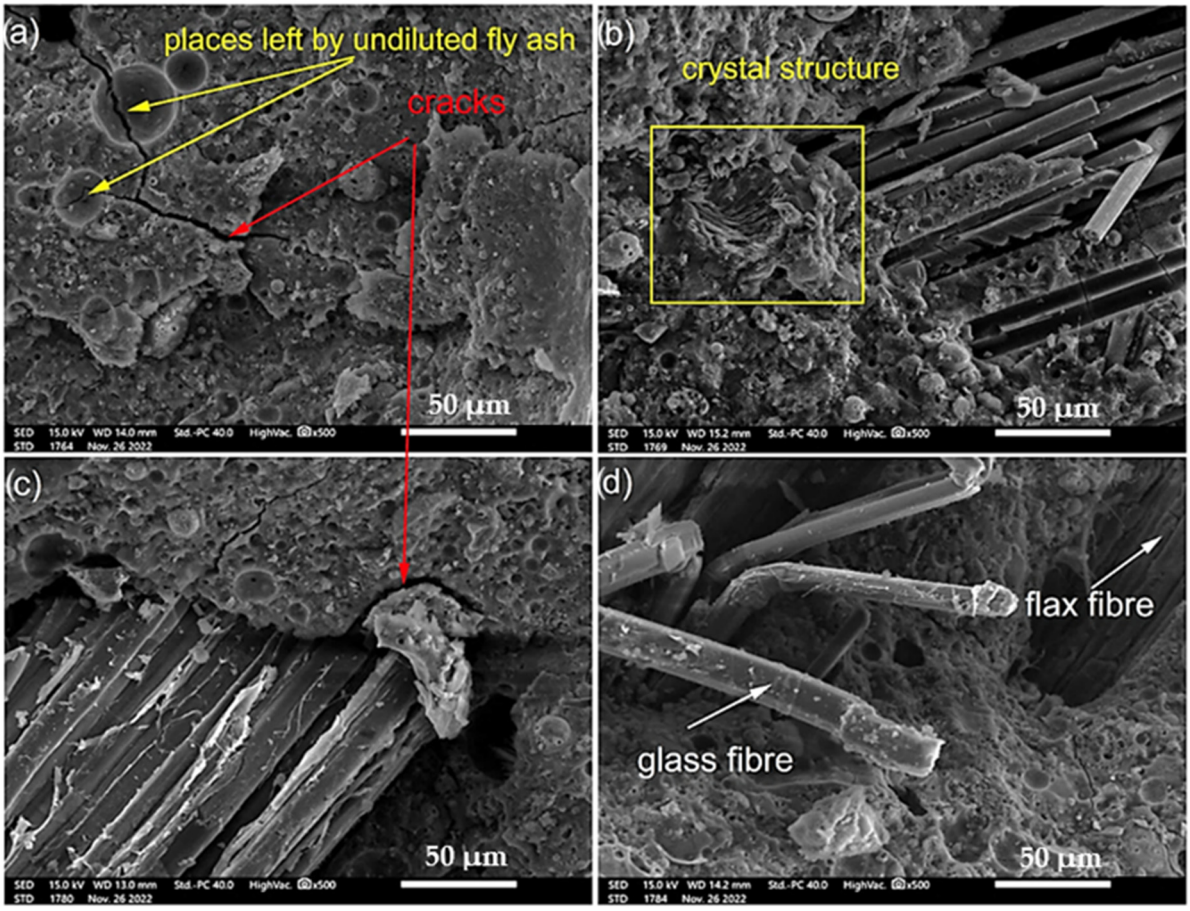

Figure 6. SEM images of the S composite: (**a**) reference specimen based on fly ash and sand, (**b**) composite with GF, (**c**) composite with FF, and (**d**) composite with hybrid reinforcement.

The microstructure of the composites in which the matrix consisted of fly ash and glass spheres (Figure 7a–d) demonstrated a different character. The deposition of glass and natural fibers and hybrid reinforcement is very similar; fiber agglomerates were visible, but the fibers were also well embedded in the geopolymer matrix. However, the matrix was characterized by significantly higher areas of undiluted fly ash particles and areas of glass bubbles.

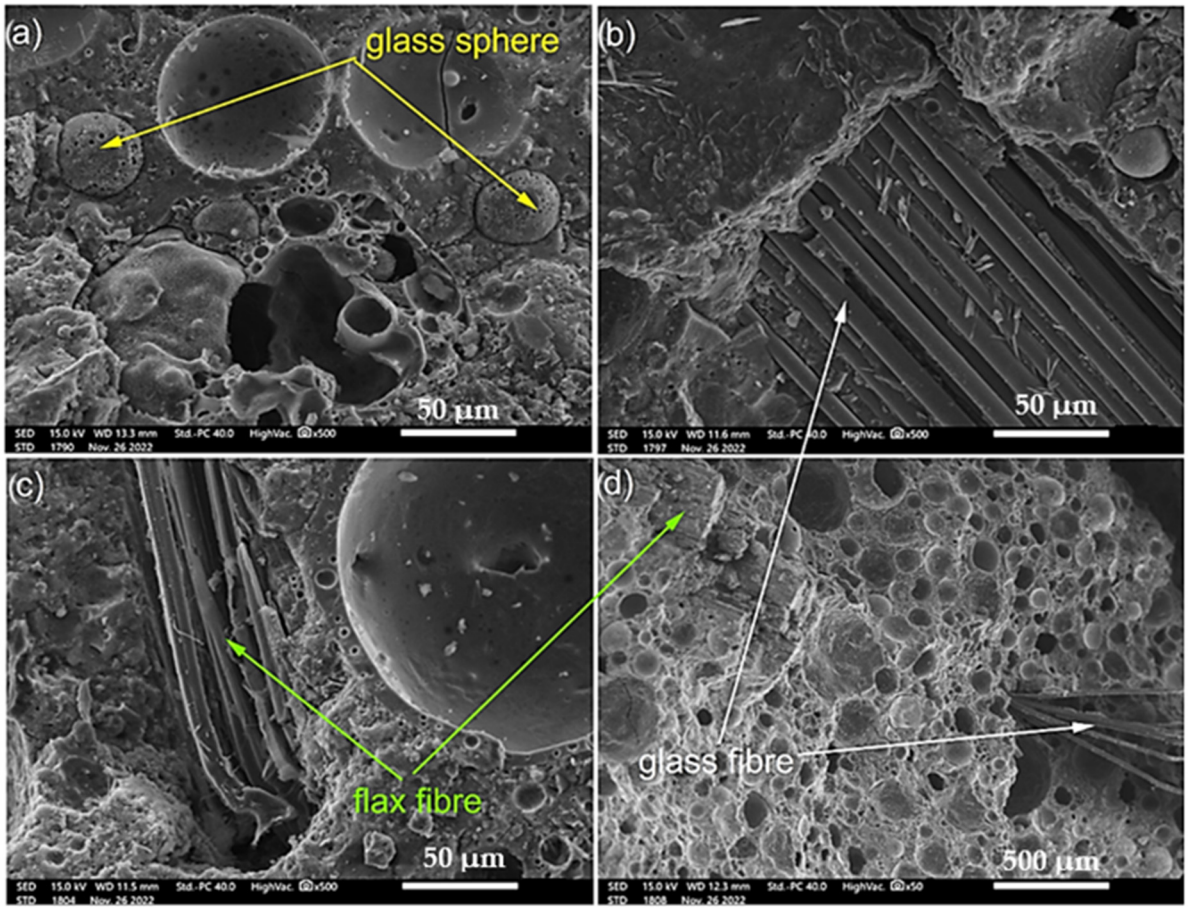

Figure 7. SEM images of the GS composite: (**a**) reference specimen based on fly ash and glass spheres (**b**) composite with GF, (**c**) composite with FF, and (**d**) composite with hybrid reinforcement.

A composite's mechanical properties depend on the interfacial bond between the fiber and the matrix. If the bond between the matrix and the fibers is too high, the fibers can be pulled out under the application of force. If the bond between the fiber and the matrix is too low, the fiber will not be able to fulfill its reinforcing role [21,54–56]. Another important aspect affecting mechanical properties is the orientation of the reinforcing fibers in relation to the applied load—randomly oriented fibers in a composite lead to poorer mechanical properties compared to fibers that are stacked [57–59]. In general, the application of fibers in geopolymers is intended to improve the mechanical properties of the overall composite, assuming that the fiber–matrix mixture is appropriately chosen.

The geopolymer composites were also subjected to thermal conductivity tests. A summary of the results is presented in Figure 8. The results demonstrated a decrease in thermal conductivity values after introducing glass fibers into the composite based on fly ash and river sand. This relationship can be attributed to the formation of voids and pores due to worse workability and the tendency to form fiber agglomerates. However, the test results for fly ash and glass sphere composites revealed the opposite effect. No significant influence of the addition of the fibers on thermal conductivity was observed. The reinforcement did not contribute to better thermal conductivity properties, as it previously slightly worsened the

measured properties. This observation confirmed the conclusion that fiber agglomeration may have a positive impact on thermal conductivity only in some cases, while in composites where the other phase is responsible for ensuring better thermal conductivity, like glass spheres, these effects are not applied. Other research studies also pointed out that the thermal conductivity properties of geopolymer materials are influenced not only by the introduced reinforcing additives but also by water content and the size, arrangement, and shape of the pores contained in the material [60–63].

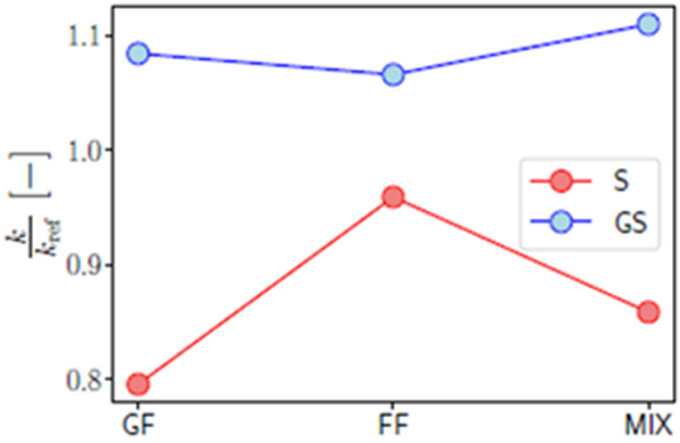

Figure 8. Thermal conductivity results of tested materials.

The list of material parameters of considered composites is presented in Table 4. The presented values are based on mean values and standard deviations. Usually, the higher values for standard deviations are connected with composites with natural fibers. It is caused by a more diverse character of fibers. Natural products are characterized by a slightly different structure and dimension than those manufactured by chemical synthesis.

Table 4. List of materials parameters of considered composites (mean values and standard deviations (STDs)).

	Sand				**Glass Sphere**			
	REF	**GF**	**FF**	**MIX**	**REF**	**GF**	**FF**	**MIX**
E_{dyn} [GPa]	12.4	10.4	10.2	11.1	4.7	4.5	4.1	5.2
STD [GPa]	0.26	0.28	0.38	0.21	0.05	0.04	0.07	0.06
ν_{dyn} [-]	0.16	0.17	0.16	0.13	0.11	0.14	0.15	0.16
STD [-]	0.01	0.03	0.03	0.00	0.01	0.01	0.03	0.02
ρ_{dyn} [kg/m^3]	1730	1680	1710	1690	910	910	980	970
STD [kg/m^3]	21	0	10	6	6	3	6	6
f_c [MPa]	45.9	37.2	38.3	41.0	18.3	17.9	17.8	20.3
STD [MPa]	2.28	1.53	0.65	1.05	1.79	1.06	0.45	0.99
σ_c [MPa]	4.42	3.53	3.64	3.73	1.63	1.43	1.71	2.03
STD [MPa]	0.12	0.32	0.09	0.27	0.10	0.11	0.02	0.15
E [GPa]	15.4	11.9	12.5	13.4	6.0	5.2	4.8	6.4
STD [GPa]	0.66	0.80	0.82	0.56	0.16	0.20	0.21	0.33
K_{Ice} [MPa· m$^{1/2}$]	0.473	0.391	0.410	0.414	0.170	0.168	0.181	0.223
STD [MPa·m$^{1/2}$]	0.028	0.069	0.025	0.024	0.004	0.007	0.009	0.019
$G_{f,1}$ [J/m^2]	8.2	7.2	7.6	7.2	2.7	3.0	4.8	4.5
STD [J/m^2]	0.69	1.95	0.76	0.65	0.15	0.34	1.26	0.79
G_f [J/m^2]	26.0	30.0	64.1	48.8	7.4	7.7	23.8	35.8
STD [J/m^2]	2.1	4.3	7.1	9.5	0.3	1.17	4.9	13.9
k [W/(m· K)]	0.906	0.721	0.869	0.778	0.273	0.296	0.291	0.303

In summary, fiber reinforcement in geopolymer materials can significantly improve the strength properties, especially in fracture behavior and limit brittle catastrophic fracture od structures. The mechanism of the reinforcement is visible in fracture toughness because the fibers join together parts of the matrix in the case of flexural strength. They give an additional force for bonding the two parts together. It is visible in this kind of force, because of the relatively low value of the fracture toughness for the matrix material. The mechanism of the reinforcement is not observed in the case of compressive strength, because in this case, the matrix material has very good properties for this kind of force, much better than natural fibers. It caused the decreasing mechanism in compressive strength to be observed. It is especially important for lightweight materials with reduced mechanical strength. Reinforcement of these kinds of materials allows for application at the same time for isolation materials that have these construction properties. It is also worth noticing that the obtained values for thermal conductivity are comparable to selected isolation materials such as aerated concrete blocks or wood (a value of about 0.2 W/(m·K)) [30].

The clear advantage of using the fibers is the improvement of the mechanical properties of the materials. Moreover, the usage of short fibers does not require changes in the technology. Both selected fibers are cost-effective. The proposed technology also has some disadvantages, including the further recycling process, and especially the application of hybrid fibers, which makes this process more complex. It is also worth noticing that the material is characterized by an environmentally friendly approach and can be used as a replacement for traditional building materials based on OPC. The alkali-activated materials are considered to be a more environmentally friendly alternative that has a lower carbon footprint and is coherent with the circular economy approach.

4. Conclusions

The presented article focuses on the mechanical, fracture, and thermal properties of geopolymer composites reinforced by flax fibers and glass fibers, both in the form of a single-type reinforcement and a hybrid connection of fibers. Two compositions were used as the geopolymer matrix: one based on fly ash and river sand, and the second containing fly ash and glass spheres. The fiber content in each case was a maximum of 1% by mass. The following conclusions can be drawn from the conducted research:

- The production of geopolymer materials modified by glass spheres reduced the compressive strength almost twice compared to the material made based on fly ash and river sand.
- The introduction of single-type fibers to the composite with river sand caused a more significant decrease in compressive strength than hybrid reinforcement.
- Single-type fibers in composites based on fly ash and glass spheres did not affect compressive strength. However, introducing hybrid reinforcement increased compressive strength by about 10% compared to the reference specimens.
- Flax fibers and hybrid reinforcement ensured higher fracture toughness and energy.
- Materials modified with glass spheres have a thermal conductivity twice as low as that of materials containing river sand.
- The introduction of single-type fibers and hybrid reinforcement slightly reduces the thermal conductivity of geopolymer materials modified with river sand, which is most likely related to the density of the material. In contrast, a slight increase in thermal conductivity characterized composites based on fly ash and glass spheres compared to the reference sample.

The presented results indicate the potential of the application of glass spheres in geopolymer materials both in terms of cracking mechanics, as a factor inhibiting brittle cracking, and in terms of reducing the thermal conductivity of materials that can be used in the construction sector, for example, for thermal panels, which should be characterized by low thermal conductivity, fire resistance, and crack resistance.

Author Contributions: Conceptualization, P.B. and K.K.; methodology, H.Š., K.S. and B.K.; software, P.N. and D.M.; validation, M.Ł., M.N. and K.S.; formal analysis, P.B., D.K. and H.Š.; investigation, P.B., D.K., D.M., M.N. and B.K.; resources, M.Ł.; data curation, P.B., M.Ł. and P.N.; writing—original draft preparation, P.B. and H.Š.; writing—review and editing, B.K., M.N. and D.K.; visualization, K.S. and P.N.; supervision, K.K.; project administration, H.Š. and K.K.; funding acquisition, H.Š. and K.K. All authors have read and agreed to the published version of the manuscript.

Funding: This work was supported by the Polish National Agency for Academic Exchange and by the Ministry of Education, Youth and Sports Czech Republic under the bilateral exchange of researchers between Poland and the Czech Republic: the grant Fibers Reinforced Geopolymers (Polish designation PPN/BCZ/2019/1/00005/U/00001, the Czech designation 8J20PL073).

Institutional Review Board Statement: Not applicable.

Informed Consent Statement: Not applicable.

Data Availability Statement: The data presented in this study are available in article.

Conflicts of Interest: The authors declare no conflicts of interest. The funders had no role in the design of the study; in the collection, analyses, or interpretation of the data; in the writing of the manuscript; or in the decision to publish the results.

References

1. Shi, C.; Fernández-Jiménez, A. Stabilization/solidification of hazardous and radioactive wastes with alkali-activated cements. *J. Hazard. Mater.* **2006**, *137*, 1656–1663. [CrossRef] [PubMed]
2. Bakharev, T. Resistance of geopolymer materials to acid attack. *Cem. Concr. Res.* **2005**, *35*, 658–670. [CrossRef]
3. Bagheri, A.; Nazari, A. Compressive strength of high strength class C fly ash-based geopolymers with reactive granulated blast furnace slag aggregates designed by Taguchi method. *Mater. Des.* **2014**, *54*, 483–490. [CrossRef]
4. Jaasrveld, J.G.S.; Deventer, J. Potential use of geopolymeric materials to immobilize toxic metals: Part I. Theory and applications. *Miner. Eng.* **1996**, *10*, 659–669.
5. Shehata, N.; Sayed, E.T.; Abdelkareem, M.A. Recent progress in environmentally friendly geopolymers: A review. *Sci. Total Environ.* **2021**, *762*, 143166. [CrossRef]
6. Chuah, S.; Duan, W.H.; Pan, Z.; Hunter, E.; Korayem, A.H.; Zhao, X.L.; Collins, F.; Sanjayan, J.G. The properties of fly ash based geopolymer mortars made with dune sand. *Mater. Des.* **2016**, *92*, 571–578. [CrossRef]
7. Agrawal, U.S.; Wanjari, S.P.; Naresh, D.N. Impact of replacement of natural river sand with geopolymer fly ash sand on hardened properties of concrete. *Constr. Build. Mater.* **2019**, *209*, 499–507. [CrossRef]
8. Venkatesan, M.; Zaib, Q.; Shah, I.H.; Park, H.S. Optimum utilization of waste foundry sand and fly ash for geopolymer concrete synthesis using D-optimal mixture design of experiments. *Resour. Conserv. Recycl.* **2019**, *148*, 114–123. [CrossRef]
9. Chen, Y.; Zhou, X.; Wan, S.; Zheng, R.; Tong, J.; Hou, H.; Wang, T. Synthesis and characterization of geopolymer composites based on gasification coal fly ash and steel slag. *Constr. Build. Mater.* **2019**, *211*, 646–658. [CrossRef]
10. Apithanyasai, S.; Supakata, N.; Papong, S. The potential of industrial waste: Using foundry sand with fly ash and electric arc furnace slag for geopolymer brick production. *Heliyon* **2020**, *6*, e03697. [CrossRef]
11. Shahedan, N.F.; Abdullah, M.M.A.B.; Mahmed, N.; Kusbiantoro, A.; Bouissi, A. Characterization of fly ash geopolymer concrete with glass bubble for thermal insulation application. *AIP Conf. Proc.* **2018**, *2030*, 020294. [CrossRef]
12. Palmero, P.; Formia, A.; Antonaci, P.; Brini, S.; Tulliani, J.M. Geopolymer technology for application-oriented dense and lightened materials. Elaboration and characterization. *Ceram. Int.* **2015**, *41*, 12967–12979. [CrossRef]
13. Zhang, Z.; Wang, K.; Mo, B.; Li, X.; Cui, X. Preparation and characterization of a reflective and heat insulative coating based on geopolymers. *Energy Build.* **2015**, *87*, 220–225. [CrossRef]
14. Chen, L.; Han, W.; Li, Z.; Wei, T.; Xiao, C. Preparation and properties of alkali stimulated geopolymer and its application in thermal insulation coating. *Adv. Mater. Res.* **2011**, *233–235*, 2443–2446. [CrossRef]
15. Kristály, F.; Szabó, R.; Mádai, F.; Debreczeni, Á.; Mucsi, G. Lightweight composite from fly ash geopolymer and glass foam. *J. Sustain. Cem. Based Mater.* **2021**, *10*, 1–22. [CrossRef]
16. Mahmood, A.; Noman, M.T.; Pechočiaková, M.; Amor, N.; Petrů, M.; Abdelkader, M.; Militký, J.; Sozcu, S.; Hassan, S.Z.U. Geopolymers and fiber-reinforced concrete composites in civil engineering. *Polymers* **2021**, *13*, 2099. [CrossRef]
17. Zuaiter, M.; El-Hassan, H.; El-Maaddawy, T.; El-Ariss, B. Properties of Slag-Fly Ash Blended Geopolymer Concrete Reinforced with Hybrid Glass Fibers. *Buildings* **2022**, *12*, 1114. [CrossRef]
18. Vijai, K.; Kumutha, R.; Vishnuram, B.G. Properties of Glass Fibre Reinforced Geopolymer Concrete Composites. *Asian J. Civ. Eng.* **2012**, *13*, 511–520.
19. Nematollahi, B.; Sanjayan, J.; Chai, J.X.H.; Lu, T.M. Properties of fresh and hardened glass fiber reinforced fly ash based geopolymer concrete. *Key Eng. Mater.* **2014**, *594–595*, 629–633. [CrossRef]

20. Archez, J.; Texier-Mandoki, N.; Bourbon, X.; Caron, J.F.; Rossignol, S. Influence of the wollastonite and glass fibers on geopolymer composites workability and mechanical properties. *Constr. Build. Mater.* **2020**, *257*, 119511. [CrossRef]
21. Ganesh, A.C.; Muthukannan, M. Development of high performance sustainable optimized fiber reinforced geopolymer concrete and prediction of compressive strength. *J. Clean. Prod.* **2021**, *282*, 124543. [CrossRef]
22. Camargo, M.M.; Taye, E.A.; Roether, J.A.; Redda, D.T.; Boccaccini, A.R. A review on natural fiber-reinforced geopolymer and cement-based composites. *Materials* **2020**, *13*, 4603. [CrossRef] [PubMed]
23. Lazorenko, G.; Kasprzhitskii, A.; Kruglikov, A.; Mischinenko, V.; Yavna, V. Sustainable geopolymer composites reinforced with flax tows. *Ceram. Int.* **2020**, *46*, 12870–12875. [CrossRef]
24. Silva, G.; Kim, S.; Castañeda, A.; Donayre, R.; Nakamatsu, J.; Aguilar, R.; Korniejenko, K.; Łach, M.; Mikuła, J. A Comparative Study of Linen (Flax) Fibers as Reinforcement of Fly Ash and Clay Brick Powder Based Geopolymers. *IOP Conf. Ser. Mater. Sci. Eng.* **2018**, *416*, 012107. [CrossRef]
25. Saccani, A.; Molari, L.; Totaro, G.; Manzi, S. Geopolymers reinforced with natural fibers: A comparison among different sources. *Appl. Sci.* **2021**, *11*, 11026. [CrossRef]
26. Korniejenko, K.; Łach, M.; Hebdowska-Krupa, M.; Mikuła, J. Impact of Flax Fiber Reinforcement on Mechanical Properties of Solid and Foamed Geopolymer Concrete. *Adv. Technol. Innov.* **2021**, *6*, 11–20. [CrossRef]
27. Correia, E.A.; Torres, S.M.; Alexandre, M.E.O.; Gomes, K.C.; Barbosa, N.P.; Barros, S.D.E. Mechanical performance of natural fibers reinforced geopolymer composites. *Mater. Sci. Forum* **2013**, *758*, 139–145. [CrossRef]
28. Silva, G.; Kim, S.; Aguilar, R.; Nakamatsu, J. Natural fibers as reinforcement additives for geopolymers—A review of potential eco-friendly applications to the construction industry. *Sustain. Mater. Technol.* **2020**, *23*, e00132. [CrossRef]
29. Asrani, N.P.; Murali, G.; Parthiban, K.; Surya, K.; Prakash, A.; Rathika, K.; Chandru, U. A feasibility of enhancing the impact resistance of hybrid fibrous geopolymer composites: Experiments and modelling. *Constr. Build. Mater.* **2019**, *203*, 56–68. [CrossRef]
30. Baziak, A.; Pławecka, K.; Hager, I.; Castel, A.; Korniejenko, K. Development and characterization of lightweight geopolymer composite reinforced with hybrid carbon and steel. *Materials* **2021**, *14*, 5741. [CrossRef]
31. Wang, Y.; Chan, C.L.; Leong, S.H.; Zhang, M. Engineering properties of strain hardening geopolymer composites with hybrid polyvinyl alcohol and recycled steel fibres. *Constr. Build. Mater.* **2020**, *261*, 120585. [CrossRef]
32. Bazan, P.; Kozub, B.; Łach, M.; Korniejenko, K. Evaluation of hybrid melamine and steel fiber reinforced geopolymers composites. *Materials* **2020**, *13*, 5548. [CrossRef] [PubMed]
33. Shaikh, F.U.A.; Patel, A. Flexural behavior of hybrid PVA fiber and AR-Glass textile reinforced geopolymer composites. *Fibers* **2018**, *6*, 2. [CrossRef]
34. Khan, M.Z.N.; Hao, Y.; Hao, H.; Shaikh, F.U.A. Mechanical properties and behaviour of high-strength plain and hybrid-fiber reinforced geopolymer composites under dynamic splitting tension. *Cem. Concr. Compos.* **2019**, *104*, 103343. [CrossRef]
35. Guo, L.; Wu, Y.; Xu, F.; Song, X.; Ye, J.; Duan, P.; Zhang, Z. Sulfate resistance of hybrid fiber reinforced metakaolin geopolymer composites. *Compos. B Eng.* **2020**, *183*, 107689. [CrossRef]
36. Torres-Martínez, L.M.; Kharissova, O.V.; Kharisov, B.I. *Handbook of Ecomaterials*; Springer: Cham, Switzerland, 2019; Volume 1. [CrossRef]
37. Kumar, S.; Mucsi, G.; Kristály, F.; Pekker, P. Mechanical activation of fly ash and its influence on micro and nano-structural behaviour of resulting geopolymers. *Adv. Powder Technol.* **2017**, *28*, 805–813. [CrossRef]
38. Nikolić, V.; Komljenović, M.; Baščarević, Z.; Marjanović, N.; Miladinović, Z.; Petrović, R. The influence of fly ash characteristics and reaction conditions on strength and structure of geopolymers. *Constr. Build. Mater.* **2015**, *94*, 361–370. [CrossRef]
39. Kocab, D.; Zitt, P.; Danek, P.; Canek, M.; Alexa, M.; Hanus, P. The influence of specimen size on the dynamic properties of lightweight concrete determined by the resonance method. *IOP Conf. Ser. Mater. Sci. Eng.* **2019**, *583*, 012028. [CrossRef]
40. *ASTM C215-19*; Standard Test Method for Fundamental Transverse, Longitudinal, and Torsional Resonant Frequencies of Concrete Specimens. ASTM International: West Conshohocken, PA, USA, 2020.
41. Frantik, P.; Masek, J. GTDiPS Software. 2015. Available online: http://gtdips.kitnarf.cz/ (accessed on 23 October 2024).
42. Stibor, M. Fracture Parameters of Quasi-Brittle Materials and Their Determination. Ph.D. Thesis, Brno University of Technology, Brno, Czech Republic, 2004.
43. Karihaloo, B.L. *Fracture Mechanics and Structural Concrete*, 1st ed.; Longman Scientific & Technical: Harlow, UK, 1995.
44. Determination of the fracture energy of mortar and concrete by means of three-point bend tests on notched beams. *Mater. Struct.* **1985**, *18*, 285–290.
45. *ČSN EN 196-1*; Methods of Testing Cement—Prat 1: Determination of Strength. ÚNMZ: Prague, Czech Republic, 2016.
46. *ASTM E1823-20b*; Standard Terminology Relating to Fatigue and Fracture Testing. ASTM International: West Conshohocken, PA, USA, 2020.
47. Korniejenko, K.; Figiela, B.; Miernik, K.; Ziejewska, C.; Marczyk, J.; Hebda, M.; Cheng, A.; Lin, W.-T. Mechanical and fracture properties of long fiber reinforced geopolymer composites. *Materials* **2021**, *14*, 5183. [CrossRef]
48. Wang, Y.; Hu, S.; He, Z. Mechanical and fracture properties of geopolymer concrete with basalt fiber using digital image correlation. *Theor. Appl. Fract. Mech.* **2021**, *112*, 102909. [CrossRef]
49. Silva, F.J.; Thaumaturgo, C. Fibre reinforcement and fracture response in geopolymeric mortars. *Fatigue Fract. Eng. Mater. Struct.* **2003**, *26*, 167–172. [CrossRef]

50. Abid, S.R.; Murali, G.; Amran, M.; Vatin, N.; Fediuk, R.; Karelina, M. Evaluation of mode II fracture toughness of hybrid fibrous geopolymer composites. *Materials* **2021**, *14*, 349. [CrossRef]
51. Lin, T.; Jia, D.; He, P.; Wang, M.; Liang, D. Effects of fiber length on mechanical properties and fracture behavior of short carbon fiber reinforced geopolymer matrix composites. *Mater. Sci. Eng. A* **2008**, *497*, 181–185. [CrossRef]
52. Lin, T.; Jia, D.; He, P.; Wang, M. In situ crack growth observation and fracture behavior of short carbon fiber reinforced geopolymer matrix composites. *Mater. Sci. Eng. A* **2010**, *527*, 2404–2407. [CrossRef]
53. Gomes, R.F.; Dias, D.P.; de Andrade Silva, F. Determination of the fracture parameters of steel fiber-reinforced geopolymer concrete. *Theor. Appl. Fract. Mech.* **2020**, *107*, 102568. [CrossRef]
54. Łach, M.; Kluska, B.; Janus, D.; Kabat, D.; Pławecka, K.; Korniejenko, K.; Guigou, M.D.; Choińska, M. Effect of Fiber Reinforcement on the Compression and Flexural Strength of Fiber-Reinforced Geopolymers. *Appl. Sci.* **2021**, *11*, 10443. [CrossRef]
55. Farhan, K.Z.; Johari, M.A.M.; Demirboğa, R. Impact of fiber reinforcements on properties of geopolymer composites: A review. *J. Build. Eng.* **2021**, *44*, 102628. [CrossRef]
56. Moujoud, Z.; Sair, S.; Ousaleh, H.A.; Ayouch, I.; Bouari, A.E.; Tanane, O. Geopolymer composites reinforced with natural Fibers: A review of recent advances in processing and properties. *Constr. Build. Mater.* **2023**, *388*, 131666. [CrossRef]
57. Shang, X.; Wang, S.; Gong, B.; Wang, y.; Li, Y.; Zhong, R. Improved carbon fibers dispersion in geopolymer composites. *Case Stud. Constr. Mater.* **2024**, *21*, e03480. [CrossRef]
58. Rahman, M.Z. Mechanical and damping performances of flax fibre composites—A review. *Compos. Part C Open Access* **2021**, *4*, 100081. [CrossRef]
59. Ranjbar, N.; Zhang, M. Fiber-reinforced geopolymer composites: A review. *Cem. Concr. Compos.* **2020**, *107*, 103498. [CrossRef]
60. Jelle, B.P.; Gustavsen, A.; Baetens, R. The path to the high performance thermal building insulation materials and solutions of tomorrow. *J. Build. Phys.* **2010**, *34*, 99–123. [CrossRef]
61. Kamseu, E.; Ngouloure, Z.N.; Ali, B.N.; Zekeng, S.; Melo, U.; Rossignol, S.; Leonelli, C. Cumulative pore volume, pore size distribution and phases percolation in porous inorganic polymer composites: Relation microstructure and effective thermal conductivity. *Energy Build.* **2015**, *88*, 45–56. [CrossRef]
62. Vucinic, D.; Miljanovic, I.; Rosic, A.; Lazic, P. Effect of Na_2O/SiO_2 mole ratio on the crystal type of zeolite synthesized from coal fly ash. *J. Serbian Chem. Soc.* **2003**, *68*, 471–478. [CrossRef]
63. Studart, A.R.; Gonzenbach, U.T.; Tervoort, E.; Gauckler, L.J. Processing routes to macroporous ceramics: A review. *J. Am. Ceram. Soc.* **2006**, *89*, 1771–1789. [CrossRef]